ACS Sustainable Chemistry & Engineering
Research Article
Cite This: ACS Sustainable Chem. Eng. 2019, 7, 17414−17423
pubs.acs.org/journal/ascecg

# Greener Terpene−Terpene Eutectic Mixtures as Hydrophobic Solvents

Mónia A. R. Martins,[†,‡,§] Liliana P. Silva,[†] Nicolas Schaeffer,[†] Dinis O. Abranches,[†]
Guilherme J. Maximo,[∥] Simão P. Pinho,[‡,§] and João A. P. Coutinho*[,†]

[†]CICECO—Aveiro Institute of Materials, Department of Chemistry, University of Aveiro, 3810-193 Aveiro, Portugal
[‡]Associate Laboratory LSRE-LCM, Department of Chemical and Biological Technology, Polytechnic Institute of Bragança, 5300-253 Bragança, Portugal
[§]Mountain Research Center—CIMO, Polytechnic Institute of Bragança, 5301-855 Bragança, Portugal
[∥]Faculty of Food Engineering, University of Campinas, 13083-862 Campinas, Brazil

*Supporting Information*

**ABSTRACT:** Natural products can be the basis for the development of green solvents, relevant for the advancement of new, more sustainable processes and products. In this work, 10 binary mixtures constituted by terpenes are prepared and characterized. Their solid−liquid phase diagrams show that room-temperature solvents can be prepared from solid terpenes in a wide composition range. These diagrams are accurately described by the conductor-like screening model for real solvents, showing it to be a useful predictive tool for the design of novel natural solvents. At the eutectic point, these mixtures possess low viscosities, densities lower than water, and high boiling temperatures. The low water solubility in the eutectic solvents together with its negligible impact on the properties measured is a strong indicator of the hydrophobic character of these mixtures. The tunable character of these mixtures is demonstrated by studying the solvatochromic parameters in the entire concentration region, the properties of the final solvents being tuned by simply varying the mole fraction of the terpenes. The high potential of this tunable character is shown in the selective extraction of dyes from their aqueous solutions. This work is expected to devise new insights concerning these solvents as well as to boost their application in green industrial processes.

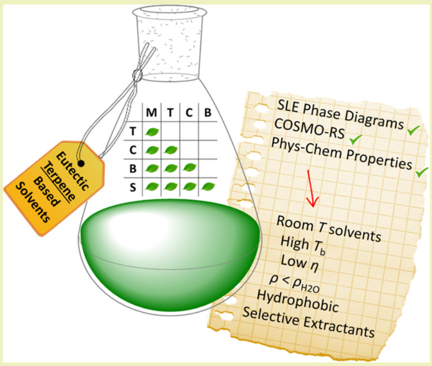

**KEYWORDS:** *terpenes, eutectic mixtures, tunable, SLE, COSMO-RS, physicochemical properties*

## INTRODUCTION

The growing importance of chemistry founded on sustainable principles has engendered a corresponding necessity in the development of sustainable solvents to further accentuate the green character of developed processes. It is estimated that 20 million MT (metric tons)[1] per annum of organic solvents are industrially produced, the majority from petroleum-based feedstock. Solvents are ubiquitous in chemistry and are applied as medium for chemical reactions, extraction processes, and cleaning processes, to name a few applications. The typically large excess of solvent to solute used results in an excessive and unsustainable consumption of nonrenewable and environmentally questionable chemicals.[2] In this context, the identification of new bio-derived organic solvents capable of replacing the volatile and toxic ones is of utmost importance.

Terpenes are a well-known class of versatile natural compounds with important applications in various fields.[3] The interesting medical properties of terpenes are extensively reported, showing that they can decrease tumor size, inhibit the growth of cancerous cells, reduce cholesterol levels, and exhibit a biocidal effect on microorganisms in vitro.[4] Additionally, terpenes are used as natural or artificial excipients, namely, as solubilizers, permeation enhancers, and natural flavorings in pharmaceutical formulations.[5] Pleasant aromas make terpenes and their mixtures essential in many commercial cleaning products, cosmetics, and perfumes.[6] In the area of fine chemicals, terpenes like myrcene were investigated as renewable alternatives to petrochemicals,[7] while Wu and Davis[8] revealed the bioconversion of algae biomass into terpenes for the production of high-energy-density aviation fuels. Due to their biodegradable character, terpenes are proposed as bio-derived alternatives to trichloroethane cleaning solvents.[9] Cymene, for example, is commonly used as a solvent for dyes and varnishes.[10] The similarity of their physicochemical properties to those of hexane makes terpenes an interesting substitute to this petroleum-based solvent.[11]

To date, mixtures of terpenes were mainly investigated in the pharmaceutical field as vehicles for transdermal delivery[12] or as analgesic, antimicrobial, and anti-inflammatory ve-

**Received:** August 7, 2019
**Revised:** September 10, 2019
**Published:** September 16, 2019

DOI: 10.1021/acssuschemeng.9b04614
ACS Sustainable Chem. Eng. 2019, 7, 17414−17423

Table 1. List of Compounds Studied along with Their Specific Rotations ($([\alpha]_D^{20})$) and Melting Properties ($T_m$ and $\Delta_m H$)

| Compound | $[\alpha]_D^{20}$ | Chemical structure | Transition[e] | $T_m$ / K | | $\Delta_m H$ / kJ·mol$^{-1}$ | |
|---|---|---|---|---|---|---|---|
| | | | | exp. | lit. | exp. | lit. |
| **L(−)-menthol**<br>2216-51-5<br>Acros Organics<br>*wt%* = 99.5[a] | -45.1[b] | 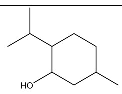 | S → L | | 315.7 ± 0.2[18] | | 12.89 ± 0.77[18] |
| **Thymol**<br>89-83-8<br>Acros Organics<br>*wt%* > 99[a] | 0 | 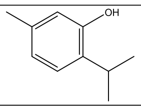 | S → L | | 323.5 ± 0.3[18] | | 19.65 ± 0.42[18] |
| **(1R)-(+)-camphor**<br>464-49-3<br>Aldrich<br>*wt%* = 98[a] | +41.1[c] | 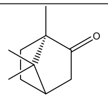 | $S_{III} \rightarrow S_{II}$<br>$S_{II} \rightarrow S_I$<br>$S_I \rightarrow L$ | 241.2 ± 0.1<br>360.8 ± 2.5<br>450.4 ± 0.4 | 242.8[19]<br>372.3[19]<br>452.7[19] | 12.68 ± 0.03<br>0.20 ± 0.01<br>5.28 ± 0.18 | 11.23[19]<br>0.15[19]<br>6.3[20] |
| **(−)-borneol**<br>464-45-9<br>Sigma-Aldrich<br>*wt%* ≥ 99[a] | -34.1[d] | 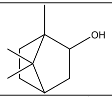 | $S_{III} \rightarrow S_{II}$<br>$S_{II} \rightarrow S_I$<br>$S_I \rightarrow L$ | 214.1 ± 1.0<br>345.7 ± 1.5<br>480.6 ± 0.1 | 213.5[19]<br>346.7[19]<br>481.6[19] | 1.15 ± 0.01<br>3.19 ± 0.09<br>7.60 ± 0.13 | 0.75[19]<br>3.03[19]<br>7.3[21] |
| ***trans*-sobrerol**<br>42370-41-2<br>Sigma-Aldrich<br>*wt%* = 99[a] | -139.3 | 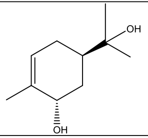 | S → L | 420.2 ± 0.4 | 423.9[22] | 27.98 ± 0.56 | 34.81[22] |

[a] Declared by the supplier. [b] Supplier: $[\alpha]_D^{20} = -51.00$. [c] Supplier: $[\alpha]_D^{25} = +44.1$. [d] Supplier: $[\alpha]_D^{20} = -35.3$. [e] S: crystalline solid, L: liquid.

hicles.[13−15] Recently, with the advent of deep eutectic solvents (DES),[16] studies involving mixtures of terpenes have been extended. Terpene-based hydrophobic eutectic solvents were proposed as extractants for metals, biomolecules, phytocannabinoids, lower alcohols, polycyclic aromatic hydrocarbons, and pesticides.[17] In a mixture, the decrease of the melting point without the formation of a new compound is a feature that increases the number of potential substances that can be used as solvents. This allows the use of terpenes with high melting points since the mixture melting temperature can be tailored with a second component. Additionally, the mixture properties can be tuned by selecting the two components and their molar ratio.

To extend the applications of these solvents to real-life scenarios, an accurate description of their solid−liquid equilibria (SLE) phase diagrams and of their physicochemical properties is of highest relevance. This allows the user to anticipate possible incompatibilities between the components, prevent manufacturing problems, and propose innovative solutions in the design of novel, more sustainable processes based on natural solvents.

In this work, binary mixtures of L(−)-menthol, thymol, (1*R*)-(+)-camphor, (−)-borneol, or *trans*-sobrerol are investigated. Their SLE phase diagrams are plotted, while the ability of conductor-like screening model for real solvents (COSMO-RS) to describe them is evaluated. This provides information on the range of compositions and temperatures for operating these systems as solvents. Fundamental liquid-phase physicochemical properties relevant to their application including densities and viscosities are reported, and the impact of the water content on the properties of the eutectic mixture is addressed. Thermogravimetric analysis (TGA) and NMR are employed to explore the structure of these mixtures, their degradation and purities, and to better appreciate the interactions of the compounds leading to the eutectic formation. The Kamlet−Taft (KT) solvatochromic parameters are investigated aiming to provide insights into the nature and characteristics of each solvent and how these characteristics can be predictively tuned through changes in the mole fraction of the eutectic components. This versatility in the solvent composition and properties was applied for dye separation, further highlighting how the separation efficiency can be tuned by manipulating the solvent composition.

## EXPERIMENTAL SECTION

**Chemicals.** Information on the compounds used in this work is summarized in Table 1 along with the observed rotatory power and melting properties. The terpenes stereochemistry is omitted in the rest of this paper. The samples were used as received from the supplier without further purification. Terpenes purity was confirmed by $^1$H and $^{13}$C NMR spectra, gas chromatography−mass spectrometry, and specific rotation. The ultrapure water used was double-distilled, passed through a reverse osmosis system, and further treated with a Milli-Q plus 185 water purification apparatus.

**Mixtures Preparation.** *Phase Diagrams.* Binary mixtures of terpenes were prepared in different proportions covering the full composition range (at 0.1 mol fraction intervals) using an analytic balance Mettler Toledo XP205. Samples were heated under stirring at a temperature 10 K above the melting temperature of the pure compound with the highest melting point, until a homogeneous liquid was formed and then stirred in the liquid state for more 30 min. After cooling at room temperature, samples of 2−5 mg were hermetically sealed in aluminum pans and weighed in a microanalytical balance AD6 (PerkinElmer, precision = 0.002 mg).

*Eutectic Mixtures.* To further characterize the systems under study, one mixture per system with a composition close to the eutectic point (Table 2) was prepared in a larger quantity, following the above procedure. The composition of the eutectic mixtures was confirmed by $^1$H NMR spectroscopy (Figure S1). Since the spectra of the mixtures match the ones from the pure compounds, it can also be concluded that no reaction between the mixtures components occurred. After melting and immediate cooling at room temperature, the mixtures were stored for 2 days to check their stability (Figure 1). In some cases, the mixtures start to become liquid even in the absence of stirring or heating, suggesting the existence of strong interactions between the components. Some systems were not considered in this study due to their high melting points (C + S and B + S) or the nonexistence of a eutectic point (C + B).

*Water-Saturated Eutectic Mixtures.* The effect of water on the physicochemical properties of the eutectic mixtures was investigated

DOI: 10.1021/acssuschemeng.9b04614
ACS Sustainable Chem. Eng. 2019, 7, 17414−17423

**Table 2. Mole Fraction ($x$) of the Binary Mixtures Close to the Eutectic Point Composition**

| | mixture components | | |
|---|---|---|---|
| abbr. | 1 | 2 | $x_1$ |
| M + T | menthol | thymol | 0.50 |
| M + C | menthol | camphor | 0.50 |
| M + B | menthol | borneol | 0.70 |
| M + S | menthol | sobrerol | 0.95 |
| T + C | thymol | camphor | 0.50 |
| T + B | thymol | borneol | 0.50 |
| T + S | thymol | sobrerol | 0.70 |
| C + B | camphor | borneol | [a] |
| C + S | camphor | sobrerol | 0.70 |
| B + S | borneol | sobrerol | 0.60 |

[a] The system C + B does not exhibit a eutectic point.

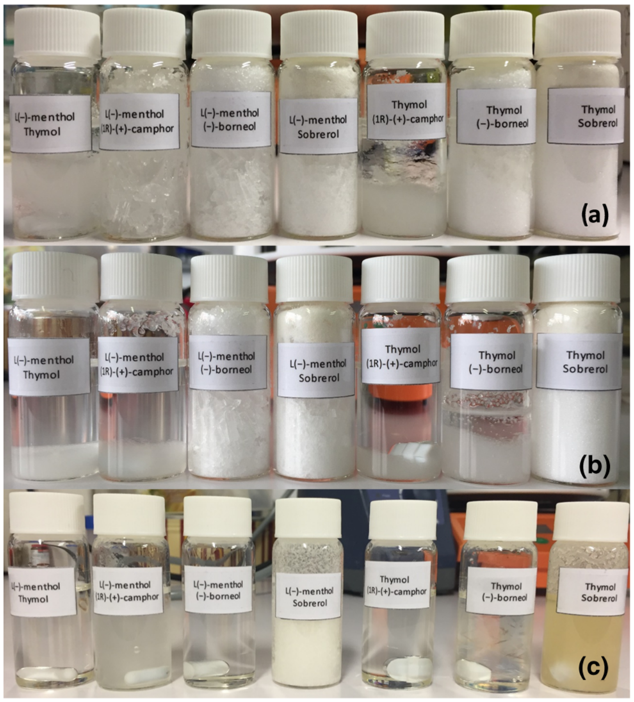

**Figure 1.** Investigated mixtures at room-temperature (compositions defined in Table 2): (a) immediately after preparation, (b) 24 h after preparation without heating or stirring, and (c) 48 h after preparation by applying 30 min stirring and heating.

here. The above-mentioned eutectic mixtures (at compositions indicated in Table 2) were mixed with ultrapure water at a 1:1 ratio. Saturation was obtained using an orbital shaker at 323.15 K and 500 rpm for 24 h. The water and organic phases were separated using a centrifuge at 5650 rpm for 30 min with phase separation achieved in all systems. Samples were kept at 323.15 K before any further measurements.

**Characterization.** *Specific Rotation.* Specific rotations of the pure terpenes were obtained in a solution of ethanol ($c$ = 10 g/100 mL) at 589 nm with an Anton Paar MCP 5100 modular circular polarimeter.

*Differential Scanning Calorimetry (DSC).* The thermal events of pure terpenes and their mixtures were obtained using a Hitachi DSC7000X working at atmospheric pressure. The equipment was previously calibrated with several standards with mass fraction purities higher than 99%. At least three cycles were performed for the pure compounds and one for the mixtures. Cooling and heating cycles were performed at 5 and 2 K $\min^{-1}$, respectively. Thermal transitions were taken as the peak temperature. In specific cases indicated in Table S1, the melting temperatures were determined: (1) with an automatic glass capillary device model M-565 from Buchi at 0.1 K $\min^{-1}$, with the solid mixtures first ground and the powder filled into a capillary tube or (2) using a visual method with an oil bath and a probe (for mixtures with a pastelike appearance). In the latter, the mixtures were gradually heated until complete melting and the temperature was controlled with a PT100 probe with a precision of ±0.1 K. The probe was previously calibrated against a calibrated platinum resistance thermometer, SPRT100 (Fluke-Hart Scientific 1529 Chub-E4), traceable to the National Institute of Standards and Technology (NIST), with an uncertainty less than $2 \times 10^{-2}$ K.

*X-ray.* The system C + B was analyzed through an X-ray powder diffractometer (Panalytical Empyrean) operating with Cu anode ($K\alpha_1$ = 1.5406 Å; $K\alpha_2$ = 1.5444 Å). The low-temperature chamber was an Anton Paar model TTK450 with temperature controller an Anton Paar TCU100; the chamber was cooled using liquid nitrogen. Diffraction data were collected in the $2\theta$ range of 10−40° in steps of 0.026 and a time per step of 50 s using a linear detector PIXEL 1D with an active length 3.347° and diffracted beams antiscatter slits of 7.5 mm.

*Thermogravimetric Analysis (TGA).* Evaporation temperatures of the eutectic mixtures of terpenes were obtained on a Setsys Evolution 1750 (SETARAM) instrument under air atmosphere at 10 K $\min^{-1}$ (precision: temperature ±0.01 K; mass ±0.01 mg).

*Kamlet−Taft Solvatochromic Parameters.* $\pi^*$, $\beta$, and $\alpha$ were measured by adding small quantities of the probes *N*,*N*-diethyl-4-nitroaniline, 4-nitroaniline, or pyridine-*N*-oxide, respectively, to the eutectic mixtures,[23,24] which were then stirred (Eppendorf Thermomixer Comfort) for 30 min at 323.15 K and 2000 rpm. $\pi^*$ and $\beta$ were quantified through the longest-wavelength absorption band using UV−vis spectroscopy (BioTeck Synergy HT microplate reader) at 323.15 K. The $\alpha$ parameter was determined by $^{13}C$ NMR, where $D_2O$ in a coaxial insert was used as solvent and trimethylsilyl propanoic acid as internal reference. At least two independent measurements were performed for each parameter and mixture.

*Density and Viscosity.* Densities and viscosities of the eutectic mixtures and the water-saturated eutectic mixtures were measured at atmospheric pressure and at different temperatures using an SVM 3001 Anton Paar viscometer (reproducibility: temperature, 0.03 K; density, 0.0001 g $cm^{-3}$; viscosity, 0.35%).

*Water Content.* The water content of pure terpenes and their eutectic mixtures at room temperature and the solubility of water in the eutectic mixtures at 323.15 K were evaluated using a Metrohm 831 Karl Fischer coulometer with Hydranal—Coulomat AG, from Riedel-de Haën.

*Nuclear Magnetic Resonance (NMR).* A Bruker Avance 300 operating at 75 MHz was used to analyze the structures of pure terpenes and their eutectic mixtures. Deuterated chloroform ($CDCl_3$) was used as solvent. The $^1H$ NMR spectra obtained confirmed the structures and mole fraction compositions of the prepared eutectic mixtures (Figure S1). Moreover, aiming to investigate the molar ratios in both phases (aqueous and organic) after the addition of water, these were also analyzed. The organic phase was analyzed using $CDCl_3$ as a solvent, and the water-rich phase was analyzed with deuterated water ($D_2O$) placed in a coaxial insert. The water peak was suppressed by using the Bruker NMR software.

**Modeling.** *Solid−Liquid Equilibria.* The phase equilibria of the eutectic mixtures with complete immiscibility in the solid phase can be described by eq 1

$$\ln(x_i \gamma_i^{l}) = \frac{\Delta_m H}{R}\left(\frac{1}{T_m} - \frac{1}{T}\right) \tag{1}$$

where $x_i$ is the mole fraction solubility of compound $i$ and $\gamma_i^{l}$ its activity coefficient in the liquid phase, $T$ is the absolute temperature, $T_m$ and $\Delta_m H$ are the melting temperature and enthalpy of the pure solute, respectively, and $R$ is the universal gas constant.[25] This is a simplified version of the solid−liquid equation, where the term related with heat capacities is neglected due to its small contribution to the

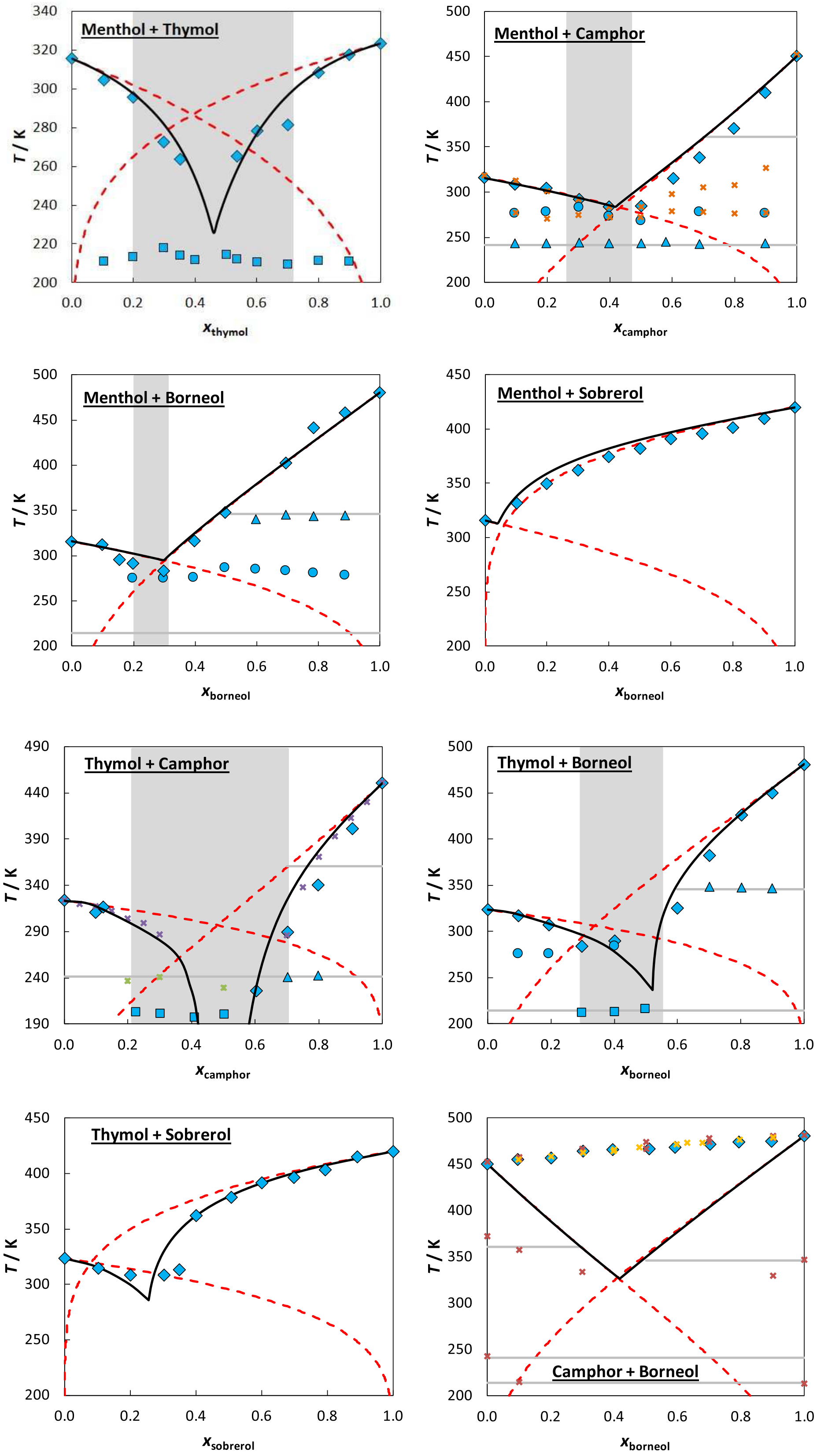

**Figure 2.** continued

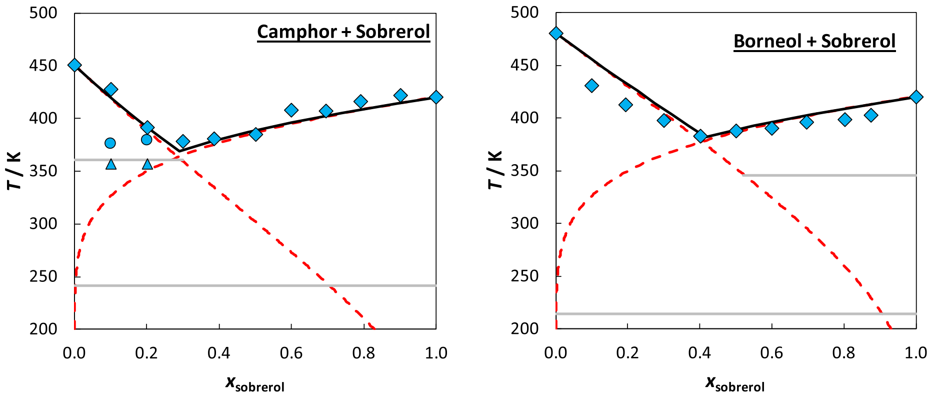

**Figure 2.** Investigated solid−liquid phase diagrams of mixtures composed of terpenes: (sky blue dimond) melting temperatures; (sky blue square), glass-transition temperatures; (sky blue circle), eutectic temperatures; (sky blue triangle up), —, pure terpenes transitions temperatures ($S_{III} \rightarrow S_{II}$, $S_{II} \rightarrow S_I$); (red hyphen), ideal solubility lines; —, COSMO-RS predictions; orange multiplication, Phaechamud et al.;[33] purple multiplication, Hrynakowski and Szmyt;[34] green multiplication, Makoś et al.;[35] red multiplication, Chandra and Murthy;[19] yellow multiplication, Vanstone.[32] The gray regions represent the concentration range for which the mixture is liquid at room temperature ($T$ = 298.15 K). M + T phase diagram is adapted from ref 36. A closer view of the C + B SLE phase diagram is provided in Figure S3.

phase equilibrium calculations.[26,27] When ideality is assumed, $\gamma_i^l = 1$ and the solubility curves can directly be derived from eq 1. Alternatively, the experimental activity coefficients can also be obtained through eq 1 using the experimental data.

*COSMO-RS.* The conductor-like screening model for real solvents (COSMO-RS) is a predictive tool for thermophysical properties and phase behavior of pure fluids and mixtures. It combines quantum chemistry with statistical thermodynamics.[28,29] COSMO-RS was used to model the phase diagrams, with all calculations performed using the software COSMOtherm, version 17.0, with the BP_TZVP_C30_1701.ctd parametrization. The $\sigma$ profiles needed as input for COSMO-RS were prepared with TURBOMOLE[30] by using the COSMO-BP-TZVP template of the software package TmoleX, version 4.2.1. This template consists on a def-TZVP basis set and a DFT with the B-P86 functional level of theory.

## ■ RESULTS AND DISCUSSION

**Solid−Liquid Phase Diagrams and COSMO-RS.** The measured phase diagrams are presented in Figure 2 along with the ideal solubility curves plotted using eq 1. Detailed experimental data are reported in Tables S1 and S2 of the Support Information, along with the activity coefficients estimated from eq 1. Due to problems in the crystallization of mixtures at some compositions of systems like M + T and T + C, only glass transitions were observed and are here reported.

The melting properties of the pure compounds used in this work are presented in Table 1 along with values from the literature. Both sets are in good agreement. Camphor and borneol present three different solid phases, and their temperatures and enthalpies of transition were also measured. This subject was also studied before by Chandra and Murthy.[19,20] Blokhin et al.[31] investigated in detail the polymorphism of the enantiopure (L-)menthol and found it to have four different polymorphs. However, in this work, only the stable $\alpha$ form was detected by DSC.

All mixtures exhibit a phase behavior characterized by a single eutectic point, with the exception of C + B, whose phase diagram indicates the existence of a solid solution in agreement with previously reported observations.[19,32] The formation of a solid solution was further confirmed by X-ray diffraction measurements at 400 K (Figure S2). Results show that the crystal structure remains unchanged (crystal structure: face-centered cubic) at different compositions as stated by Chandra and Murthy.[19] The mixture forms a continuous solid solution in phase $S_I$, which is an orientationally disordered phase.[19]

The SLE phase diagrams of mixtures M + S, M + C, M + B, C + S, and B + S present weak deviations from the ideal behavior, suggesting that hydrogen-bonding networks established in these systems are not significantly different from those present in the pure compounds. On the other hand, mixtures involving thymol (M + T,[36] T + C, T + B, and T + S) present strong negative deviations from ideality. The system M + T was studied in detail by us.[36] The nonideality was attributed to a strong hydrogen bond established between the acidic proton of the phenolic hydroxyl of thymol, and the oxygen of the hydroxyl group of menthol, resulting in much stronger interactions compared to the pure compounds.[36] The study of the M + T system allowed the identification of a new class of eutectic mixtures forming true deep eutectic systems, designated as type V DES.[36] The strong negative deviations from ideality lead to phase diagrams with regions where the melting points of the mixtures are close to, or below, their glass-transition temperatures. In particular, for mixtures M + T, T + C, and T + B, this results in a very large liquidus region.

In the literature, SLE phase diagrams of M + C, T + C, and C + B were previously reported.[19,32−35] However, some experimental techniques used are not advisable due to the non-negligible vapor pressure of these compounds,[21,22] potentially resulting in incorrect phase diagrams, as shown in Figure 2. The data obtained by Phaechamud et al.[33] for the system M + C underestimate the melting temperatures in the camphor-rich side. The same is observed for the data reported by Makoś et al.[35] for the system T + C. The experimental points measured by Hrynakowski and Szmyt[34] for T + C and by Chandra and Murthy[19] and Vanstone[32] for C + B are in good agreement with the data measured in this work.

COSMO-RS was used to predict the phase diagrams. As can be seen in Figure 2, this tool is able to successfully describe the SLE of the mixtures, making COSMO-RS a useful tool for the a priori screening and design of terpenes mixtures. The only exception found is in the C + B system whose phase diagram indicates the existence of a solid solution. It is important to highlight the ability of COSMO-RS to correctly describe the nonideal behavior of the mixtures containing thymol. The average deviations between COSMO-RS predicted temperatures and experimental data are reported in Table S3 and are in the range of 5−18 K.

The melting point depressions for most of the investigated mixtures are considerably large, but only a few are liquid at room temperature in a wide composition range, even when both pure compounds are solid. This represents a big advantage since it increases the flexibility of the relative amounts that can be used, depending on the desired physical state and properties of the final product.

In the next sections, the sustainability and applicability of the investigated systems will be evaluated at the mixture eutectic composition (excepting C + B) studying relevant properties and features.

**Thermogravimetric Analysis.** TGA was used to find upper-temperature limits at which these systems can be used (Table 3) without significant mass losses. Thermograms were obtained by measuring the mass loss under heat conditions in an open system (Figure S4). This is related to evaporation or sublimation of the compounds and not to their degradation as previously stated.[37] Pure components and their mixtures show similar mass loss patterns with a single-step decay with the exception of C + S and B + S that present a second plateau. This is attributed to interactions between the pure components that cause different evaporation temperatures. For these two cases, no further analysis is performed.

**Table 3. TGA Parameters of the Investigated Systems**

| system | $x_1$ | $T_{\text{onset}}$/K | $T_{\text{peak}}$/K |
|---|---|---|---|
| menthol | | 421.34 | 458.30 |
| thymol | | 434.44 | 473.69 |
| camphor | | 438.57 | 457.07 |
| borneol | | 428.57 | 471.72 |
| sobrerol | | 456.21 | 501.96 |
| M + T | 0.50 | 451.78 | 488.24 |
| M + C | 0.50 | 405.08 | 447.52 |
| M + B | 0.70 | 438.99 | 472.82 |
| M + S | 0.95 | 418.58 | 459.21 |
| T + C | 0.50 | 437.44 | 480.81 |
| T + B | 0.50 | 416.75 | 461.47 |
| T + S | 0.70 | 451.39 | 515.40 |

The mass loss $T_{\text{onset}}$ ranges from 405 to 456 K corresponding to M + C and pure sobrerol, respectively. In most cases, mixtures presenting an ideal behavior have $T_{\text{onset}}$ lower than or between that of their pure constituents. M + B is an exception, where $T_{\text{onset}}$ of the mixture is higher than that of pure menthol and borneol. With the exception of T + B, mixtures involving thymol (i.e., mixtures with a nonideal behavior) have $T_{\text{peak}}$ higher than their individual constituents, suggesting the formation of azeotropes. Although there are no VLE data to confirm this hypothesis, such behavior is consistent with the negative deviations observed in the SLE phase diagrams.

Mixtures involving thymol present a higher operational temperature limit. This is very interesting since these mixtures present large negative deviations from ideality, i.e., a large melting point depression and a wide range of temperature and compositions where the mixtures are in the liquid state. These results are very relevant for industrial applications. Together with the phase diagrams, they establish boundary limits in which to apply these mixtures with minimal evaporation losses or crystallization.

**Kamlet−Taft Solvatochromic Parameters.** Most reactions occur in solution, with the solvent properties influencing its suitability as a reaction or extraction medium. The Kamlet−Taft parameters $\pi^*$, $\beta$, and $\alpha$ give information about the polarizability/dipolarity, hydrogen-bond acceptor, and donor capacity of the mixtures, thereby providing an insight into the nature and characteristics of each solvent. These were here measured at 323.15 K and are presented in Figure 3 and Table S4 (equations available in Supporting Information). At this temperature, only pure menthol and thymol are in the liquid state and thus these are the only pure terpenes for which it was possible to measure the KT parameters: menthol[18] $\beta$ = 0.66; $\pi^*$ = 0.42; $\alpha$ = 0.53 and thymol $\beta$ = 0.13; $\pi^*$ = 0.99; $\alpha$ = 1.02. The systems C + S and B + S were not considered here due to the high melting temperatures of their eutectic mixtures.

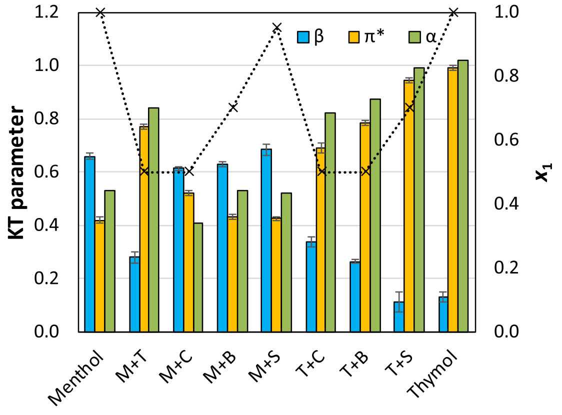

**Figure 3.** Kamlet−Taft solvatochromic parameters of the mixtures at 323.15 K. Clustered columns correspond to the KT parameters (left *y*-axis), while the dotted line corresponds to the mole fraction of either thymol or menthol (right *y*-axis).

From Figure 3, mixtures involving thymol present high polarizability/dipolarity as observed before for mixtures of menthol/thymol with monocarboxylic acids.[18] This is related to the presence of the aromatic ring in the thymol structure.[18] Moreover, $\pi^*$ increases with the increase of thymol content in the mixture. Conversely, for mixtures containing menthol, $\pi^*$ decreases with the increase of menthol content. T + S is the mixture that presents the highest polarizability/dipolarity due to the high content on thymol ($x_{\text{thymol}}$ = 0.70).

As observed in our previous work,[18] the variation observed for parameter $\beta$ is the opposite of parameter $\alpha$. Mixtures with menthol present a higher capacity to accept hydrogen bonds that increases with the menthol content in the mixture. The capacity to act as a hydrogen-bond donor, $\alpha$, is higher in mixtures with thymol. This is in line with what has been discussed above about the acidity of thymol hydroxyl proton.

Mixtures involving camphor display the lowest values of $\alpha$ since this ketone does not have the capacity to donate hydrogen bonds according with the sigma profile computed by COSMO-RS (Figure S5). These profiles suggest that sobrerol and thymol have the larger capacity to donate hydrogen bonds (higher $\alpha$), followed by menthol. On the other hand, camphor (closely followed by borneol and menthol) seems to be the compound with larger capacity to accept hydrogen bonds and thus should have a higher $\beta$. This is in agreement with the experimental KT parameters measured.

DOI: 10.1021/acssuschemeng.9b04614
ACS Sustainable Chem. Eng. 2019, 7, 17414−17423

When comparing the mixtures evaluated here with common molecular solvents (Table S4), it can be seen that mixtures with thymol present higher $\pi^*$ values than organic solvents, meaning a higher ability to establish nonspecific interactions with a solute. Additionally, thymol-based mixtures also show hydrogen-bond acidity, whose values are in general higher than alcohols, ketones, alkanes, and aromatics solvents. The ability to accept protons of the studied mixtures is similar to that of common alcohols and higher than that of water.

More importantly, as shown in Figure 3, mixtures of two terpenes can produce different combinations on the values of $\pi^*$, $\beta$, and $\alpha$, due to the different characteristics of each solvent that can be tailored for specific applications. Aiming at exploring this topic, the KT solvatochromic parameters of the mixtures M + T and T + C were measured as a function of the mole fraction, as shown in Figure 4. In both systems, the parameters $\pi^*$ and $\alpha$ increase with the increase of molar fraction of thymol while $\beta$ shows the opposite behavior covering wide ranges of these parameters. This shows how the desired properties of the final solvent can be tailored based on the mole fraction of the constituents rather than using always the eutectic point composition or a well-defined molar ratio.

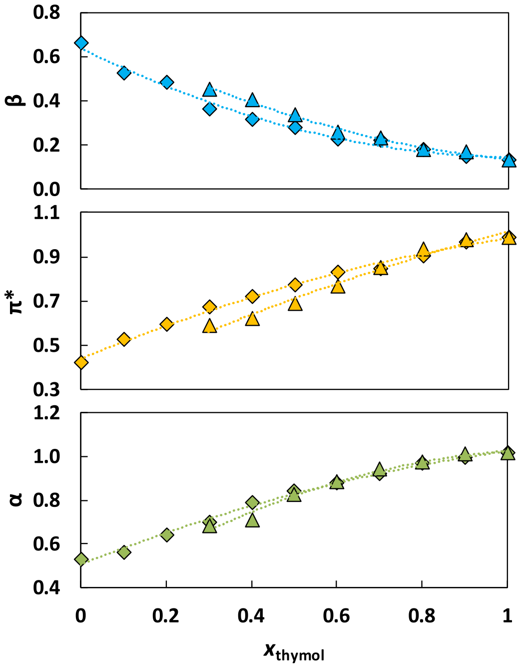

**Figure 4.** Kamlet−Taft solvatochromic parameters of the mixtures ◆ M + T and ▲ T + C at 323.15 K as a function of thymol mole fraction. The dotted lines are a guide to the eyes.

**Densities and Viscosities.** To minimize mass transfer limitations, an ideal solvent should have a low viscosity, and for extraction purposes, its density should be sufficiently different from the water density to ease phase separation. Here, these physicochemical properties were investigated aiming to evaluate the applicability of the mixtures under study.

Densities and viscosities of the terpene-based mixtures at the eutectic composition, both dry and water-saturated, were measured at atmospheric pressure in the temperature range of 278.15−373.15 K. The results are displayed in Figures S6 and S7 and listed in Tables S5−S8. The water content of pure terpenes and their mixtures is presented in Table S9. Systems T + S, C + S, and B + S were not considered here due to the high melting temperatures of their eutectic points. Densities and viscosities of pure thymol and menthol were previously reported by us.[38]

All systems measured present densities lower than water. Viscosities decrease with the addition of water, while densities increase in the same conditions. As observed for mixtures with monocarboxylic acids,[18] mixtures containing thymol present higher densities than those with menthol. The density of pure menthol is lower than the densities of any of the mixtures considered at all temperatures, while the density of pure thymol is in between the density of T + C and T + B. Regarding viscosities, pure thymol presents lower viscosities than all of the mixtures studied. At moderate and high temperatures, viscosities are very low and similar. At 298.15 K, viscosities vary from 16 to 110 mPa corresponding to M + C and M + B. By adding water, these values decrease to 15 and 74 mPa with water contents of around 2200 and 17 000 ppm (without and with water saturation, respectively). Due to its lower value and despite the increase in the water content after the saturation of the mixture, the viscosity of the system M + C remains approximately constant.

Osch et al.[37] reported values for water content, density, and viscosity of the system M + T (1:1): 306.8 ppm (295.15 K), 0.9366 g cm$^{-3}$ (298 K), and 53.14 mPa s (298 K), respectively. Significant differences were obtained here for the water content (3059 ppm) and, consequently, for viscosity (38.08 mPa s). This may be attributed to the stereoisomer of menthol used. Here, L(−)-menthol (CAS: 2216-51-5) was used while authors used a racemic mixture dl-menthol (CAS: 89-78-1).

When in equilibrium with water, some of the eutectic mixture will partition to the water phase and, as reported in Table S9, a certain quantity of water will solubilize in the eutectic mixture. The water content of the pure compounds and their mixtures with and without saturation with water varies between 79 and 23 545 ppm (Table S9), increasing after the saturation with water due to the solubility of water in the mixture. However, the solubility of water in the eutectic mixtures is in general low (12 209−23 545 ppm), demonstrating the hydrophobic character of these binary mixtures.

$^1$H NMR analysis of the eutectic systems and water phases after mutual saturation was performed, and the results are reported in Figure S8. The mole ratio of the pure compounds in the organic phase is, after mixing with water, the same as the original. After saturation, the water peak (≈1.56 ppm) is visible in the systems M + C and M + B. The water phase was evaluated by suppressing the water peak. The ratio of the terpenes in the aqueous phase was evaluated for the systems M + T, M + C, and T + C. The changes observed from the original composition are in line with the solubilities of the pure terpenes in water. For instance, the composition prepared for the M + T system was 0.5:0.5, and after equilibrium, the ratio of terpenes in the aqueous phase was estimated to be 0.13:0.87 due to the higher solubility of thymol in water, $9.84 \times 10^{-4}$ g/g$_{H_2O}$, compared to the solubility of menthol, $6.27 \times 10^{-4}$ g/g$_{H_2O}$.[39,40] The system M + C is apparently an exception since the terpenes ratio in the water phase does not correspond to the relative solubility of the pure terpenes in water. This can be attributed to the NMR accuracy. For the other systems, no isolated peaks could be assigned to the components of the mixtures, preventing the analysis in the aqueous phase.

Summarizing, the viscosities of the mixtures investigated are slightly greater than that of conventional organic solvent but significantly less than those of ionic DES. Furthermore, the reported densities are sufficiently different from the water density, indicating that these systems can be interesting options for industrial applications. Additionally, the water solubility on these mixtures is quite low, thus showing a low ability to absorb water from the atmosphere, or during extraction processes.

**Tailored Extraction.** The properties of the proposed eutectic solvents can be selectively tuned changing the components as well as their respective composition. In this section, this flexibility in the eutectic properties was applied to the selective separation of two dyes, *N*,*N*-diethyl-4-nitroaniline and chloranilic acid, from its mixture in water. Eutectic mixtures were contacted with the dyes aqueous solution. The organic-to-aqueous phase ratio was 1, and the volume of each phase remained constant after extraction. The detailed experimental equations are available in the Supporting Information. The extraction of the respective dyes and their mutual separation is shown in Figure 5. An example of the UV−vis spectra of the aqueous and eutectic phases before and after extraction is presented in Figure S9. Results indicate a good separation with *N*,*N*-diethyl-4-nitroaniline (yellow) (1) that is quantitatively extracted to the organic phase for all compositions (distribution ratio $D_{N,N\text{-diethyl-4-nitroaniline}} = 100$ − assuming quantitative extraction). In contrast, the extraction of chloranilic acid (purple) (2) is strongly influenced by the terpene selection as well as by the molar composition of the eutectic formulation. The extraction of chloranilic acid to the eutectic phases varies from 14 to 49% from M + T (0.3:0.7) to M + C (0.5:0.5), respectively. Additionally, as observed for the system M + T, the selectivity (S) almost tripled by changing the mole fraction of the compounds in the terpene mixture. An effective separation was obtained with a maximum separation factor of around 600 when using 70% of thymol in the eutectic mixture.

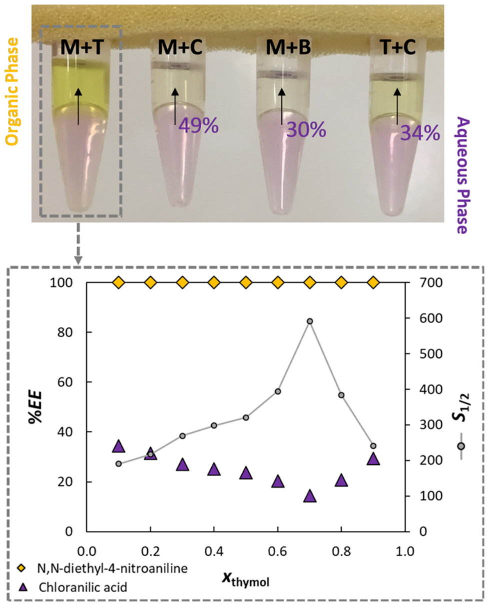

**Figure 5.** Separation of dyes *N*,*N*-diethyl-4-nitroaniline (1-yellow) and chloranilic acid (2-purple) in mixtures of terpenes and water.

Aiming at the design of green solvents to be used in industry, a wide variety of terpene-based eutectic mixtures were prepared and characterized. The SLE phase diagrams were measured in the whole composition range showing significant melting point depression. Liquid solvents can be obtained for some of these mixtures in a wide composition and temperature range. The COSMO-RS was shown to be able to predict the phase behavior of these mixtures, including the systems of thymol with remarkable strong negative deviations from ideality. This model can thus be used to design new eutectic mixtures. The eutectic mixtures present high boiling temperatures, densities lower than water, and low viscosities—important parameters when envisioning industrial applications. The solubility of water in the eutectic systems is quite low, and it has a low impact on the properties measured, demonstrating the hydrophobic character of these mixtures and preventing their loss and contamination to the aqueous phase.

The solvatochromic parameters show that the mixtures with menthol present a higher capacity to accept hydrogen bonds while the capacity to act as a hydrogen-bond donor is higher in mixtures with thymol. More importantly, the characteristics of the final solvent can be tailored since different mixtures give different combinations of $\pi^*$, $\beta$, and $\alpha$.

This flexibility in the solvent characteristics was applied to the selective and tunable separation of dyes from water, where changes in the eutectic components and their mole fraction affect the separation factor. No volume change is observed for the different systems reinforcing the idea that a total separation of the organic and water phases occurs and attesting to the hydrophobic character of the systems investigated. It was also proved that the extraction and selectivity can be manipulated by varying the mole fraction of the terpenes in the mixture.

## ■ ASSOCIATED CONTENT

### Ⓢ Supporting Information

The Supporting Information is available free of charge on the ACS Publications website at DOI: 10.1021/acssuschemeng.9b04614.

> NMR spectra of pure terpenes and their mixtures; experimental SLE phase diagrams data and activity coefficients; X-ray diffractogram of C + B; AAD between COSMO-RS predictions and experimental data; TGA thermograms; KT solvatochromic parameters and equations; sigma profiles of pure terpenes; densities and viscosities; water contents; and NMR spectra of aqueous and organic phases after equilibrium (PDF)

## ■ AUTHOR INFORMATION

### Corresponding Author

*E-mail: jcoutinho@ua.pt. Tel: +351 234401507. Fax: + 351 234370084.

### ORCID

Mónia A. R. Martins: 0000-0003-0748-1612
Liliana P. Silva: 0000-0002-6636-1920
Nicolas Schaeffer: 0000-0002-0747-2532
Guilherme J. Maximo: 0000-0002-3252-3004
Simão P. Pinho: 0000-0002-9211-857X
João A. P. Coutinho: 0000-0002-3841-743X

### Notes

The authors declare no competing financial interest.

## ■ ACKNOWLEDGMENTS

This work was developed in the scope of the project CICECO—Aveiro Institute of Materials POCI-01-0145-

FEDER-007679 (UID/CTM/50011/2019) and Associate Laboratory LSRE-LCM (UID/EQU/50020/2019), funded by national funds through FCT/MCTES (PIDDAC). FCT is also acknowledged for funding the project DeepBiorefinery (PTDC/AGRTEC/1191/2014). M.A.R.M. acknowledges the financial support from NORTE-01-0145-FEDER-000006—funded by NORTE2020 through PT2020 and ERDF. L.P.S. acknowledges FCT for her Ph.D. grant SFRH/BD/135976/2018. G.J.M. acknowledges the national funding agencies CNPq (305870/2014-9, 309780/2014-4, 140702/2017-2, 406918/2016-3, 406963/2016-9), FAPESP (2014/21252-0, 2016/08566-1), and FAEPEX/UNICAMP (0125/16).

## REFERENCES

(1) Clark, J. H.; Farmer, T. J.; Hunt, A. J.; Sherwood, J. Opportunities for Bio-Based Solvents Created as Petrochemical and Fuel Products Transition towards Renewable Resources. *Int. J. Mol. Sci.* **2015**, *16*, 17101−17159.

(2) Clarke, C. J.; Tu, W.-C.; Levers, O.; Bröhl, A.; Hallett, J. P. Green and Sustainable Solvents in Chemical Processes. *Chem. Rev.* **2018**, *118*, 747−800.

(3) Zwenger, S.; Basu, C. Plant Terpenoids: Applications and Future Potentials. *Biotechnol. Mol. Biol. Rev.* **2008**, *3*, 1−7.

(4) Davis, A. Topical Pharmaceutical Compositions, EP Patent No. EP3073991A1, 2013.

(5) Balbani, A. P. S.; Stelzer, L. B.; Montovani, J. C. Pharmaceutical Excipients and the Information on Drug Labels. *Braz. J. Otorhinolaryngol.* **2006**, *72*, 400−406.

(6) Tetali, S. D. Terpenes and Isoprenoids: A Wealth of Compounds for Global Use. *Planta* **2019**, *249*, 1−8.

(7) Behr, A.; Johnen, L. Myrcene as a Natural Base Chemical in Sustainable Chemistry: A Critical Review. *ChemSusChem* **2009**, *2*, 1072−1095.

(8) Wu, W.; Davis, R. W. One-Pot Bioconversion of Algae Biomass into Terpenes for Advanced Biofuels and Bioproducts. *Algal Res.* **2016**, *17*, 316−320.

(9) Brown, L. M.; Springer, J.; Bower, M. Chemical Substitution for 1,1,1-Trichloroethane and Methanol in an Industrial Cleaning Operation. *J. Hazard. Mater.* **1992**, *29*, 179−188.

(10) Corma, A.; Iborra, S.; Velty, A. Chemical Routes for the Transformation of Biomass into Chemicals. *Chem. Rev.* **2007**, *107*, 2411−2502.

(11) Yara-Varón, E.; Selka, A.; Fabiano-Tixier, A. S.; Balcells, M.; Canela-Garayoa, R.; Bily, A.; Touaibia, M.; Chemat, F. Solvent from Forestry Biomass. Pinane a Stable Terpene Derived from Pine Tree Byproducts to Substitute n-Hexane for the Extraction of Bioactive Compounds. *Green Chem.* **2016**, *18*, 6596−6608.

(12) Gala, U.; Pham, H.; Chauhan, H. Pharmaceutical Applications of Eutectic Mixtures. *J. Dev. Drugs* **2013**, *2*, 1−2.

(13) Stott, P. W.; Williams, A. C.; Barry, B. W. Transdermal Delivery from Eutectic Systems: Enhanced Permeation of a Model Drug, Ibuprofen. *J. Controlled Release* **1998**, *50*, 297−308.

(14) Yong, C. S.; Oh, Y.-K.; Jung, S. H.; Rhee, J.-D.; Kim, H.-D.; Kim, C.-K.; Choi, H.-G. Preparation of Ibuprofen-Loaded Liquid Suppository Using Eutectic Mixture System with Menthol. *Eur. J. Pharm. Sci.* **2004**, *23*, 347−353.

(15) Kang, L.; Jun, H. W.; McCall, J. W. Physicochemical Studies of Lidocaine-Menthol Binary Systems for Enhanced Membrane Transport. *Int. J. Pharm.* **2000**, *206*, 35−42.

(16) Abbott, A. P.; Capper, G.; Davies, D. L.; Rasheed, R. K.; Tambyrajah, V. Novel Solvent Properties of Choline Chloride/Urea Mixtures. *Chem. Commun.* **2003**, *99*, 70−71.

(17) Dwamena, A. K.; Dwamena, K. A. Recent Advances in Hydrophobic Deep Eutectic Solvents for Extraction. *Separations* **2019**, *6*, 9.

(18) Martins, M. A. R.; Crespo, E. A.; Pontes, P. V. A.; Silva, L. P.; Bülow, M.; Maximo, G. J.; Batista, E. A. C.; Held, C.; Pinho, S. P.; Coutinho, J. A. P. Tunable Hydrophobic Eutectic Solvents Based on Terpenes and Monocarboxylic Acids. *ACS Sustainable Chem. Eng.* **2018**, *6*, 8836−8846.

(19) Chandra, G.; Murthy, S. S. N. Dielectric and Thermodynamic Study of Camphor and Borneol Enantiomers and Their Binary Systems. *Thermochim. Acta* **2018**, *666*, 241−252.

(20) Rietveld, I. B.; Barrio, M.; Veglio, N.; Espeau, P.; Tamarit, J. L.; Céolin, R. Temperature and Composition-Dependent Properties of the Two-Component System d- and l-Camphor at 'Ordinary' Pressure. *Thermochim. Acta* **2010**, *511*, 43−50.

(21) Štejfa, V.; Fulem, M.; Růžička, K.; Červinka, C. Thermodynamic Study of Selected Monoterpenes II. *J. Chem. Thermodyn.* **2014**, *79*, 272−279.

(22) Bettinetti, G.; Giordano, F.; Fronza, G.; Italia, A.; Pellegata, R.; Villa, M.; Ventura, P. Sobrerol Enantiomers and Racemates: Solid-State Spectroscopy, Thermal Behavior, and Phase Diagrams. *J. Pharm. Sci.* **1990**, *79*, 470−475.

(23) Schneider, H.; Badrieh, Y.; Migron, Y.; Marcus, Y. Hydrogen Bond Donation Properties of Organic Solvents and Their Aqueous Mixtures from 13 C NMR Data of Pyridine-n-Oxide. *Z. Phys. Chem.* **1992**, *177*, 143−156.

(24) Teles, A. R. R.; Capela, E. V.; Carmo, R. S.; Coutinho, J. A. P.; Silvestre, A. J. D.; Freire, M. G. Solvatochromic Parameters of Deep Eutectic Solvents Formed by Ammonium-Based Salts and Carboxylic Acids. *Fluid Phase Equilib.* **2017**, *448*, 15−21.

(25) Prausnitz, J. M.; Lichtenthaler, R. N.; Azevedo, E. G. *Molecular Thermodynamics Fluid Phase Equilibria*; Prentice-Hall, 1986.

(26) Gmehling, J.; Kolbe, B.; Kleiber, M.; Rarey, J. *Chemical Thermodynamics for Process Simulation*; Wiley-VCH, 2012.

(27) Coutinho, J. A. P.; Andersen, S. I.; Stenby, E. H. Evaluation of Activity Coefficient Models in Prediction of Alkane Solid-Liquid Equilibria. *Fluid Phase Equilib.* **1995**, *103*, 23−39.

(28) Klamt, A. Conductor-like Screening Model for Real Solvents: A New Approach to the Quantitative Calculation of Solvation Phenomena. *J. Phys. Chem. A* **1995**, *99*, 2224−2235.

(29) Klamt, A. *COSMO-RS From Quantum Chemistry to Fluid Phase Thermodynamics and Drug Design*; Elsevier: Amsterdam, The Netherlands, 2005.

(30) TURBOMOLE. *A Development of University of Karlsruhe and Forschungszentrum Karlsruhe GmbH, 1989-2013*; TURBOMOLE GmbH, 2007. http://www.turbomole.com/.

(31) Štejfa, V.; Bazyleva, A.; Fulem, M.; Rohlíček, J.; Skořepová, E.; Růžička, K.; Blokhin, A. V. Polymorphism and Thermophysical Properties of L- and DL-Menthol. *J. Chem. Thermodyn.* **2019**, *131*, 524−543.

(32) Vanstone, E. LXXVI.—The Miscibility of Solids. *J. Chem. Soc., Trans.* **1909**, *95*, 590−604.

(33) Phaechamud, T.; Tuntarawongsa, S.; Charoensuksai, P. Evaporation Behavior and Characterization of Eutectic Solvent and Ibuprofen Eutectic Solution. *AAPS PharmSciTech* **2016**, *17*, 1213−1220.

(34) Hrynakowski, K.; Szmyt, M. Die Heterogenen Gleichgewichte in Zweistoffsystemen Mit Thymol Als Einer Komponente. *Arch. Pharm.* **1935**, 273, 418−427.

(35) Makoś, P.; Przyjazny, A.; Boczkaj, G. Hydrophobic Deep Eutectic Solvents as "Green" Extraction Media for Polycyclic Aromatic Hydrocarbons in Aqueous Samples. *J. Chromatogr. A* **2018**, *1570*, 28−37.

(36) Abranches, D. O.; Martins, M.; Silva, L.; Schaeffer, N.; Pinho, S. P.; Coutinho, J. A. P. Phenolic Hydrogen Bond Donors in the Formation of Non-Ionic Deep Eutectic Solvents: The Quest for Type V DES. *Chem. Commun.* **2019**, *55*, 10253−10256.

(37) Van Osch, D. J. G. P.; Dietz, C. H. J. T.; Van Spronsen, J.; Kroon, M. C.; Gallucci, F.; Van Sint Annaland, M.; Tuinier, R. A Search for Natural Hydrophobic Deep Eutectic Solvents Based on Natural Components. *ACS Sustainable Chem. Eng.* **2019**, *7*, 2933−2942.

(38) Martins, M. A. R.; Carvalho, P. J.; Palma, A. M.; Domańska, U.; Coutinho, J. A. P.; Pinho, S. P. Selecting Critical Properties of

Terpenes and Terpenoids through Group-Contribution Methods and Equations of State. *Ind. Eng. Chem. Res.* **2017**, *56*, 9895−9905.

(39) Martins, M. A. R.; Silva, L. P.; Ferreira, O.; Schröder, B.; Coutinho, J. A. P.; Pinho, S. P. Terpenes Solubility in Water and Their Environmental Distribution. *J. Mol. Liq.* **2017**, *241*, 996−1002.

(40) Ajisaka, N.; Hara, K.; Mikuni, K.; Hashimoto, H. Effects of Branched Cyclodextrins on the Solubility and Stability of Terpenes. *Biosci., Biotechnol., Biochem.* **2000**, *64*, 731−734.